Synthesis of Polypropylene/Clay Nanocomposites Using Bisupported Ziegler-Natta Catalyst

Ahmad Ramazani S. A., Fahimeh Tavakolzadeh, Hossein Baniasadi

Polymer Group, Department of Chemical and Petroleum Engineering, Sharif University of Technology, Tehran, Iran

Received 23 December 2008; accepted 14 July 2009
DOI 10.1002/app.31102
Published online 27 August 2009 in Wiley InterScience (www.interscience.wiley.com).

ABSTRACT: In this article, preparation of polypropylene/clay nanocomposites (PPCNC) via *in situ* polymerization is investigated. $MgCl_2$/montmorillonite bisupported Ziegler-Natta catalyst was used to prepare PPCNC samples. Montmorillonite (MMT) was used as an inert support and reinforcement agent. The nanostructure of the composites was characterized by X-ray diffraction, scanning electron microscopy, and transmission electron microscopy techniques. Obtained results showed that silica layers of the MMT in these PPCNC were intercalated, partially exfoliated, and uniformly dispersed in the polypropylene matrix. Thermogravimetric analysis showed good thermal stability for the prepared PPCNC. Differential scanning calorimetric was used to investigate both melting and crystallization temperatures, as well as the crystallinity of the PPCNC samples. Results of permeability analysis showed significant increase in barrier properties of PPCNC films. Effective parameters on molecular weight and flow ability of produced samples such as Al/Ti molar ratio and H_2 concentration were also investigated. © 2009 Wiley Periodicals, Inc. J Appl Polym Sci 115: 308–314, 2010

Key words: poly(propylene); clay; nanocomposites; Ziegler-Natta polymerization

INTRODUCTION

Polymers have been successfully reinforced by glass fiber and other inorganic materials. In these conventional composites, the polymer and additives are not homogeneously dispersed and are in non-nanometric levels. If nanometer dispersion could be achieved, both mechanical and thermal properties as well as barrier properties might be further improved or new unexpected features might appear.[1] The effect of additives in nanometeric size generally corresponds to very large relative surface areas and strong interactions between these particles and the polymer matrix.[2,3] Polymer/inorganic nanocomposites are one of the most important groups of synthetic engineering materials. These new materials possess the advantages of both organic materials, such as lightweight, flexibility, and good mold ability and inorganic materials, such as high strength, heat stability, and chemical resistance.[4] Among the polymer/inorganic nanocomposites, polymer-layered silicate nanocomposites because of their enhanced physical and mechanical properties including barrier, flammability resistance, ablation performance, environmental stability, and solvent resistance have received so much interaction.[1,3] Smectite type clays such as montmorillonite (MMT) are most commonly layered silicate used for production of polymer-layered silicate nanocomposites. Several methods have been introduced for the production of polymer/clay nanocomposites including, melt blending, solution intercalation, and *in situ* polymerization.[4,5] The first and second methods have been successfully used for producing many polymeric matrix containing polar groups. However, these promising approaches are not suitable for preparation of polyolefin/clay nanocomposites.[6,7] Polyolefin are nonpolar organic materials which cannot be easily intercalated between the clay layers.[6,8,9] To improve the compatibility of clay and polyolefins, alkyl-ammonium surfactants have been used to modify smectite type clays such as MMT. It was found that the thermal degradation of ammonium alkyl surfactants at high processing temperatures ($200 \pm 10^{\circ}C$), not only accelerated the aging and decomposition of polyolefins but also led to the restacking of the silicate layers.[5,10]

In situ polymerization has been recently considered as alternative method for exfoliation of clay in clay containing polyolefin nanocomposites.[5,11] In this method, by polymerization of the monomer between the clay layers, the silicate layers can exfoliate and disperse uniformly in polymeric matrix. Polypropylene is one of the most widely used polymeric materials. However production of polypropylene/clay nanocomposites (PPCNC) via an intercalative

Correspondence to: A. Ramazani S. A. (Ramazani@sharif.edu).

© 2009 Wiley Periodicals, Inc.

polymerization process has been found only in few literatures. Ma et al.[12] reported preparation of PPCNC by organoclay and $MgCl_2$ supported Ziegler-Natta catalyst. Hwu et al.[2] reported production of PPCNC using metallocene catalyst supported on organomodified clay.

However, production of PPCNC with unmodified clay using Ziegler-Natta catalysts with *in situ* process has not been reported yet in the literatures. So, to find a practical and an efficient way for production of such nanocomposites, in this article, production of polypropylene/clay nanocomposite with nonorganomodified clay using *in situ* polymerization of propylene monomers by $MgCl_2$/MMT bisupported Ziegler-Natta catalysts is investigated.

MATERIALS AND METHODS

Materials

Sodium montmorillonite (Kunipa, with about 115meq/100 gr CEC) was supplied from Kunimine industries company and untreated bentonite (mineral clay) was supplied from Tabriz mine. Propylene (polymerization grade) was supplied by Arak petrochemical company and was purified by passing through columns of 4A type molecular sieves. Titanium tetrachloride ($TiCl_4$ > 99% purity, Riedel), magnesium ethoxide ($Mg(OEt)_2$ 95% purity, Fluka), and Dibutyl phthalate (ID, internal donor) (Merk) were used for preparation of catalyst. Triethyl aluminum (TEA) ($AlEt_3 \sim 15\%$ in hexane, Fluka), triisobutyl aluminum (TIBA) [$Al(iBu)_3$ > 96% purity, Merck] were used after diluting in hexane. Toluene and *n*-hexane were used after refluxed over Na for 24 h under Argon for drying. Dimethoxy methyl cyclohexyl silane was obtained from Arak petrochemical company and use as an external donor.

Catalyst preparation

Before activation, clay was calcined for 6 h at 400°C to eliminate surface absorbed water and bound water. The latter type of water which is associated in a geometric structure around the cations, is found between the sheet layers of smectites. The calcined MMT and $Mg(OEt)_2$ with different weight ratios were introduced into a catalyst preparation reactor that equipped with a stirrer and oil bath and was purged with high purity Argon. Table I shows weight ratios of $Mg(OEt)_2$ to MMT used for catalyst preparation. Subsequently, 200 mL toluene was added to the system and the temperature of the reactor was increased to 80°C while stirrings. $TiCl_4$ (20 mL) and electron donor (ID) (2 mL) were added to the slurry. The temperature was increased to 115°C and at this temperature the slurry was stirred for 2 h. The obtained product was washed with toluene three times and then toluene (200 mL) and $TiCl_4$ (20 mL) were added. The slurry was stirred for 4 h at 115°C. The final product was washed 10 times by hexane at 40°C. This catalyst can be used in suspension form or after drying under Argon atmosphere.

TABLE I
Clay Types and Weight Ratios of Clay to Magnesium Ethoxide for Preparing the Catalysts

Catalyst name	$Clay/Mg(OEt)_2$ (Weight ratio)	Clay type
Cat. 1	1/1	Mineral MMT
Cat. 2	2/1	
Cat. 3	3.5/1	
Cat. 4	4/1	
Cat. 5	5/1	
Cat. 6	2/1	Kunipa
Cat. 7	5/1	

In situ coordinated polymerization

Polymerization experiments were carried out in a Buchi reactor in slurry phase. Hexane is used as a diluent in all experiments. Reactor was degassed and purified with Argon at 90°C before charging by 500 mL hexane. Subsequently, TIBA or TEA, which act as cocatalyst, external donor, catalyst, and hydrogen were added to the reactor. When the reactor reached to the predetermined temperature, propylene monomer was introduced to the reactor. Propylene was supplied under a pressure of 1 to 4 bars to maintain the polymerization for a certain period of time. After predetermined reaction time, polymerization was terminated with diluted HCl solution of ethanol. The composite dried in a vacuum oven at 60°C for 5 h. The pure PP was also prepared using a conventional Ziegler-Natta catalyst in the same polymerization conditions, as a counterpart reference of the nanocomposites.

During polymerization, the small propylene molecules could easily diffuse in the clay galleries and polymerize with produced catalyst complex to form polypropylene chains. The size of the polypropylene macromolecular chains is about several hundreds of nanometer, far than the gallery space of the clay. Therefore, the layer structure of the clay could be destroyed by growing PP macromolecular chains and uniformly exfoliated in PP matrix.[12]

Characterization

Wide angle X-ray diffraction (XRD) analysis was performed on a Philips PW 1800 with Cu Kα radiation ($\lambda = 0.1504$ nm) at a generator voltage of 40 kV

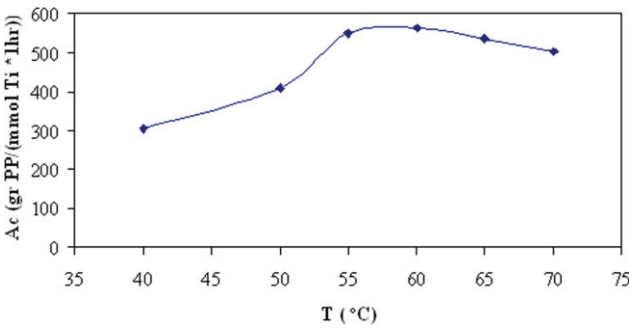

Figure 1 Effects of the polymerization temperature on the catalyst activity, $P = 4$ bar, Al/Ti = 38, $H_2 = 0.1$ bar, Cat. 7. [Color figure can be viewed in the online issue, which is available at www.interscience.wiley.com.]

and generator current of 100 mA. The interlayer spacing (d_{001}) of produced polypropylene/clay nanocomposite samples was calculated in accordance with Bragg's equation: $2d\sin\theta = n\lambda$.

Differential scanning calorimetry (DSC) tests were conducted using a Perkin Elmer Pyris IDSC thermal analyzer under nitrogen atmosphere with heating rate of 10°C/min. All scans were recorded in temperatures in the range of 23–250°C and sample weights were between 10 and 15 mg.

Transmission electron microscopy (TEM) tests were carried out on a Philips-CM200-FEG transmission electron microscope (as verified by EDX) using an acceleration voltage of 150 kV. The sample was ultramicrotomed with a diamond knife on a Leica Ultracur UCT microtome at room temperature to give 70–nm-thick section.

The morphology of the fractured surfaces of the samples was investigated using a XL30 Philips scanning electron microscope (SEM). An SPI sputter coater was used to sputter-coat the fractured surfaces with gold for enhanced conductivity.

The titanium content of clay supported catalysts was measured using ICP/AES standard method.

The thermal behavior was studied using a Perkin-Elmer (STA 1500) thermogravimitric analyzer (TGA) at a heating rate of 10°C/min to 600°C under air flow. Permeability measurements were done using a set-up based on the ASTM D1434.

Isotactic index (II) measurements were carried out in boiling heptanes for 10 h using a soxhlet's extractor.

The molecular weight (MW) and its polydispersity of PP were measured using gas permission chromatography (GPC; Waters Alliance GPC2000) in 1,2,4-trichlorobenzene at 140°C and column flow rate of 0.3 mL/min. Separation of PP from powdery PP/MMT nanocomposites was conducted by soxhlet extraction using O-dichlorobenzene as the solvent.

Melt flow index (MFI) measured based on the ASTM method D 1238-57T (230°C, 2.16 kg).

RESULTS AND DISCUSSIONS

Effects of polymerization temperature

Polymerization temperature varied from 40 to 70°C limited by the boiling point of the solvent. Figure 1 shows polymerization temperature effects on the activity of the catalyst [Ac; gr PP/(mmol Ti*1 h)]. The activity of the catalyst increased when the polymerization temperature was raised from 40 to 60°C. As seen in Figure 1, at 60°C the activity of catalyst reaches to its maximum values. So this temperature could be considered as the best one for polymerization of propylene monomers in this system. Decreasing in the activity of the catalyst at above 60°C could be attributed to increasing of transfer and termination side reactions and also reduction of monomer solubility in hexane diluent.[13]

Effects of H_2 concentration

Addition of hydrogen to the reactor of olefin monomer polymerization with Ziegler-Natta catalysts is a widely used industrial method to control polymer flow ability and molecular weights.[14] It has been experimentally observed, that the activity of the heterogeneous catalyst increases when the propylene polymerization is carried out in the presence of molecular hydrogen. This fact has been explained by considering that the hydrogen chain transfer reactions would renew "dormant" sites in the catalyst, coming from isolated secondary insertions.[14,15] Table II shows the effect of H_2 on the polymerization behavior of the catalyst. This table shows that by increasing the amount of H_2 concentration, the catalyst productively increased. Usual explanation for this behavior is that H_2 activates some dormant sites in the catalyst as mentioned above. Another

TABLE II
Data of Polymerization, Produced Catalyst and PPCNCs, $T_P = 60$°C, $P = 4$ bar

Catalyst name	Al/Ti molar ratio	H_2 (bar)	Ac (gr PP/(mmol Ti*1 h)	Cocatalyst
Cat. 1	17	0	210[a]	TEA
	17	0.1	230[a]	
	17	0.3	280[a]	
	10	0.1	200[a]	
Cat. 2	17	0.1	182[a]	
Cat. 3	17	0.1	110[a]	
	9.6	0.1	110	
	9.6	0.1	170	TIBA
Cat. 4	9.6	0.1	130	
	12	0.1	172	
Cat. 5	35	0.1	297	
Cat. 6	35	0.1	257	
Cat. 7	35	0.1	525	

[a] Ac (gr PP/(mmol Ti*0.5 h).

TABLE III
Effect of H_2, and Al/Ti Molar Ratio on MW, T_P = 60°C, P = 4 bar, Cat. 1, Cocatalyst; TEA, 0.5 h, 1.6 wt % Clay

H_2 (bar)	Al/Ti molar ratio	MFI	Mw	PDI	II
0	17	3.5	253,885	3.63676	98.82
0.1	17	15	101,909	5.17036	99.2
0.1	10	7	206,360	4.27398	99

hypothesis can be based on the oxidation of Ti^{2+} sites that are not active for polymerization of propylene. By addition of H_2, the oxidation of the Ti^{2+} sites to Ti^{3+} sites may take place that can easily polymerize propylene monomer. Table III shows the effect of H_2 on the MFI of prepared PPCNC. As shown in this table, the MFI of the samples was considerably affected by H_2 presence during polymerization. It could be attributed to increasing in chain-transfer reactions which results in decreasing in MW.[16] Figure 2 also shows the effect of the H_2 on the molecular weight of the samples. As shown in Figure 2, by increasing in H_2 content the molecular weight obviously decreased.

Effects of cocatalyst

Cocatalyst could also have important effects on the polymerization behavior. Figure 3 shows the effects of the Al/Ti molar ratio on the polymerization activity. This figure shows that as the Al/Ti molar ratio increases, the activity of catalyst increases. Such behavior is in agreement with previously presented data in literature and can be attributed to the overall reduction of active sites at high concentration of cocatalyst.[6] Also, at constant Al/Ti molar ratio the activity of prepared catalyst from Kunipa clay, i.e. Cat. 7, is higher than the activity of prepared catalyst from mineral clay, i.e. Cat. 5. The presented results in Table II also show that TIBA has more activity than TEA, which may lie in the low reduction capability of TIBA.[6] Figure 2 shows the effects

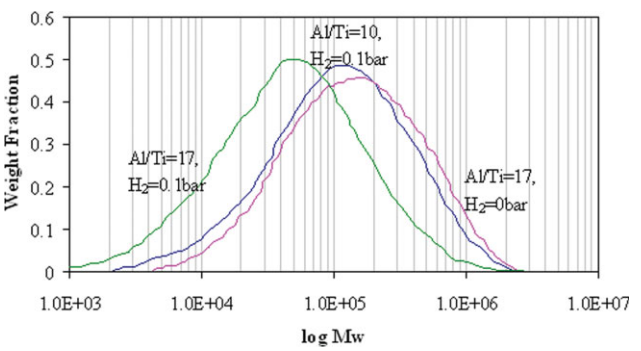

Figure 2 GPC curves for prepared PPCNC 1.6 wt %. [Color figure can be viewed in the online issue, which is available at www.interscience.wiley.com.]

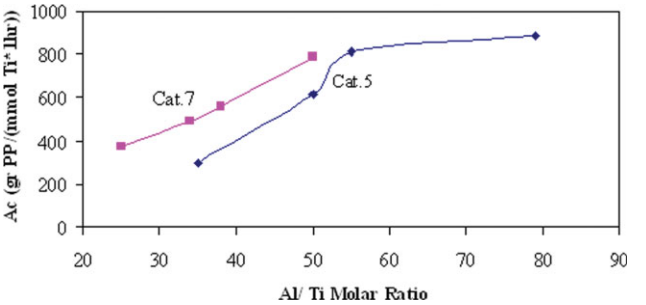

Figure 3 Effect of Al/Ti molar ratio on polymerization activity, Cocatalyst: TIBA, T_P = 60°C, P = 4 bar, TIBA, H_2 = 0.1 bar. [Color figure can be viewed in the online issue, which is available at www.interscience.wiley.com.]

of cocatalyst and hydrogen concentrations on the molecular weight of the produced samples. This figure shows that by increasing in Al/Ti molar ratio the molecular weight of the samples decreases. The average molecular weight of the prepared PPCNC varied from 100,000 to 260,000 depends on the H_2 concentration and Al/Ti molar ratio. The molecular weight disparity of PP vary from 3.6 to 5.17 (see Table III), showing that the active complex must be multisites.

Isotactisity index

The amount of atactic polypropylene content in prepared PPCNC was measured by soxhlet's extraction method. After washing with a suitable solvent for atactic PP in an extractor, all the soluble species were removed, leaving only the silicate layers and insoluble PP which were more than 98% (Table III).

XRD and TEM of PPCNC

The XRD patterns of MMT, prepared catalyst, and prepared PPCNC (2 wt % clay) are shown in Figure 4. Presented XRD shows that the (001) diffraction peak of clay (Kunipa) appears at $2\theta = 7.6°$

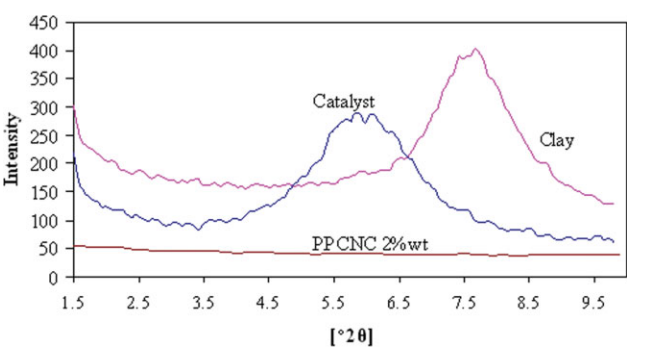

Figure 4 XRD pattern of clay, supported clay, and PPCNC 2 wt %. [Color figure can be viewed in the online issue, which is available at www.interscience.wiley.com.]

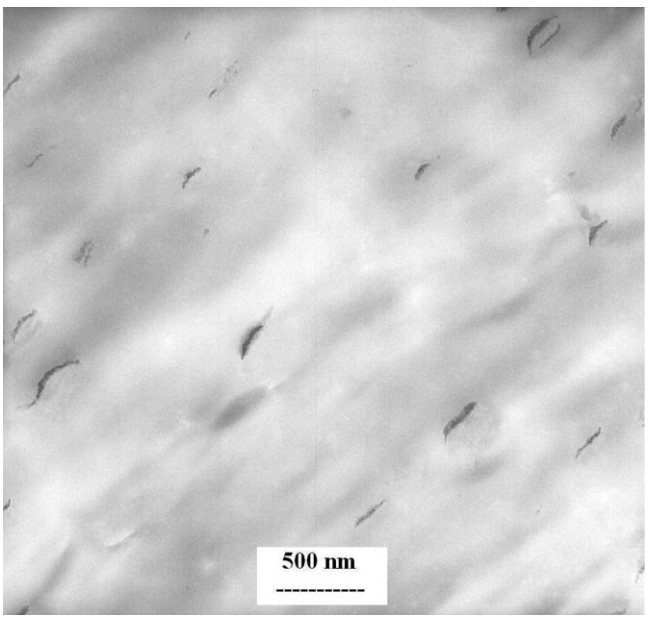

Figure 5 TEM micrograph of a thin section of PPCNC having 2 wt % of clay.

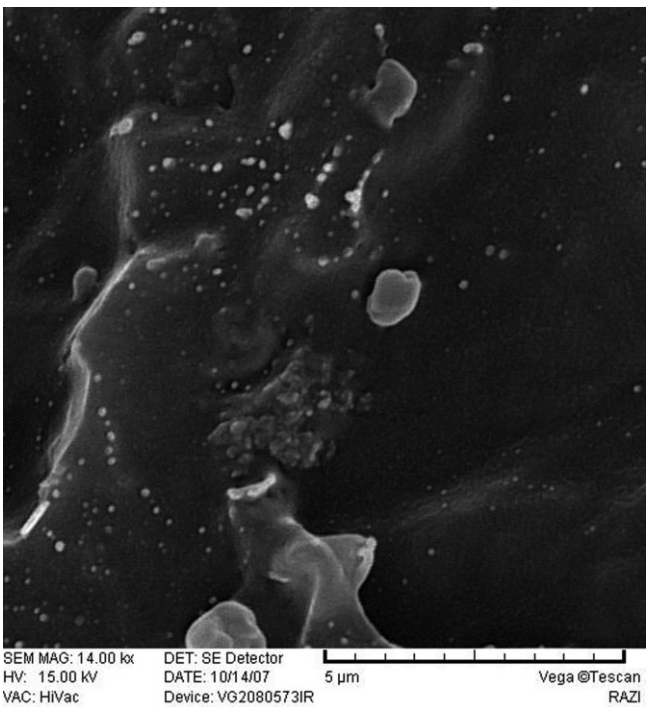

Figure 6 SEM image of fractured surface of PPCNC with 2 wt % clay.

and for prepared catalyst this peak shifts to a smaller angle. This indicates that supporting the catalyst on the clay could result in an increase in the interlayer spacing of the clay layers. This characteristic peak of the MMT disappeared in XRD pattern of PPCNC, indicating that the average interlayer spacing of the clay layers in PPCNC increased and is larger than that can be detected by using XRD instrument. These results show that clay layers should be mostly exfoliated in the polymeric matrix after polymerization of the monomers between the silicate layers.

Dispersion of the clay layers in prepared samples have been observed using TEM. The ultrathin slides prepared by sectioning the injection-molded samples along with the direction perpendicular to the injection. Figure 5 displays the TEM images of a thin section of PPCNC having 2 wt % of the clay. As seen, the dark lines represent intersections among the silicate layers of MMT and each silicate sheet is randomly dispersed into the PP matrix following polymerization of the monomers by the bisupported catalyst.

SEM

The morphology of the prepared PPCNC was examined by observing SEM images prepared from fracture surface of samples. Figure 6 shows the SEM image of PPCNC with 2 wt % clay content. Results indicate that the fractured surface of the samples are relatively fine and smooth and without large holes and knots. This indicates not only a good dispersion of clay but also a good adhesion between PP and clay layers.

DSC analysis

Crystallization and melting temperatures and enthalpies for the different PPCNC samples obtained from DSC spectra are revealed in Table IV. As seen in this table, one can determine that these PPCNCs have melting temperatures higher than pure PP, and have substantially higher crystallization temperatures but less crystallization enthalpies or degree of crystallinity. Higher melting temperature in produced PPCNC can be attributed to the slow heat transfer through the composites.[17] This result is consistent with other reported data in the literatures.[17,18]

The crystallinity of the samples was calculated from the enthalpy evolved during crystallization and melting using the following equations[19,20]:

TABLE IV
Thermal Properties of PP and PP/clay Nanocomposites Formed from Polymerization of Propylene with Industrial Catalyst and Clay Supported One

Clay content (wt %)	T_c (°C)	ΔH_m (J/g)	T_m (°C)	ΔH_c (J/g)	X1%	X2%
0	108.322	100	161.775	−99.010	60.0	60.6
2	121.524	102	167.149	−99.171	61.3	61.8
5	119.855	98	166.681	−91.206	58.1	59.3
7	111.015	87	163.500	−81.245	52.9	52.7

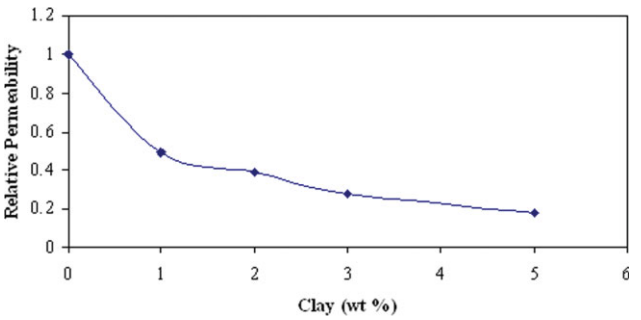

Figure 7 Relative permeability of the PPCNCs samples. [Color figure can be viewed in the online issue, which is available at www.interscience.wiley.com.]

$$X1\% = (\Delta H_c/((1-\varphi)\times \Delta H_f^{\circ})100\% \quad (1)$$

or

$$X2\% = (\Delta H_f/\Delta H_f^{\circ})\times 100\% \quad (2)$$

where X1 and X2 are crystallinity of the samples, ΔH_c is the apparent enthalpy of crystallization, ΔH_f is the heat of the fusion determined by DSC, ΔH_f° is the value of the enthalpy corresponding to the melting of 100% crystalline sample, and φ is the weight fraction of the filler in the nanocomposite. A value of 165 J/g was chosen for ΔH_f°.[19–21]

The nanoscale MMT layers affect the crystallization in two opposite ways. The nucleation of MMT could relatively increase the number of crystallite, whereas crystallization degree could slightly decrease because of movement hindering of polymer chains by MMT layers. The restricted chains might not crystallize. Therefore, the relative crystallization degree decreases with increasing MMT content in the PPCNC.[6]

Permeability measurement

For investigating of the clay dispersion in polymer/clay nanocomposites, permeability measurements can also be used. The exfoliated intercalated polymer/clay nanocomposites are those where the layered clay plates are delaminated and dispersed in the polymeric matrix. In intercalated and exfoliated state individual clay plates will have the highest possible aspect ratio and thus the highest barrier improvement is expected. The gas permeability of the nanocomposites can reduce to almost a half to one-third of that of the unfilled polymer even at low clay content. This effect could be explained by tortuous path model, developed by Neilson[1] in which the platelets obstruct the passage of gases and other permeates through the matrix polymer. The barrier improvement is predicted by this model to be a function of the volume fraction of plates, φ, and a function of the aspect ratio of the plates, α, with higher aspect ratios providing greater barrier improvement according to the flowing equation for permeability:

$$P_{\text{nanocomposite}} = \frac{(1-\varphi)P_{\text{matrix}}}{1+\alpha\varphi/2} \quad (3)$$

where $P_{\text{nanocomposite}}$ represents the permeability of the resulting nanocomposite and P_{matrix} represents the permeability of the polymer matrix.[1]

Figure 7 shows the relative permeability of the PPCNCs samples to pure PP. It can be seen that by increasing the clay content, the permeability decreased. At higher clay concentration, dependence of permeability to clay content reduces. This can be described by Neilson model. The height of the clay platelet, witch is about 1 nm, is dictated by the crystal structure of platelet and the width is 10–300 nm, then the maximum aspect ratio of the clay layers is about 300 nm. In this case, at any volume fraction there is a maximum relative permeability that can be achieved. For example at 5 volume fraction, the minimum relative permeability at $\alpha = 300$ is about 0.11. So the obtained diagram for permeability usually has an exponential form. Reduction of relative permeability to one-fifth for samples with less than 3 percent clay (Fig. 7) shows that the must of the clay layers must be exfoliated.

TGA analysis

The obtained results from thermogravimetric analysis of the prepared PPCNCs are shown in Figure 8. Results from TGA show that by introducing the clay into the PP matrix the thermal stability considerably increase. Enhancement in thermal stability of the polymer/clay nanocomposites is attributed to the lower permeability of oxygen and the diffusibility of the degradation products from the bulk of the polymer caused by the exfoliated clay in the composites.[19,22,11]

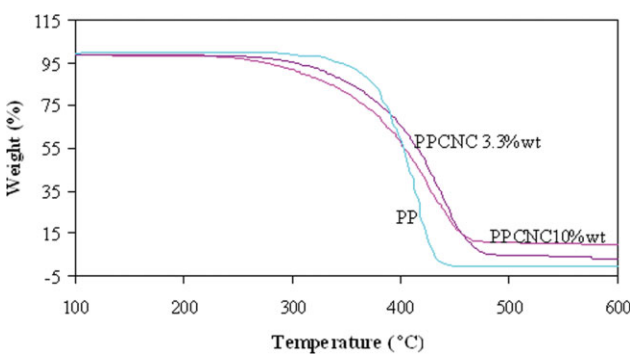

Figure 8 TGA curves of PP and PPCNC 3.3% and PPCNC 10%. [Color figure can be viewed in the online issue, which is available at www.interscience.wiley.com.]

Presented results in Figure 8 show that thermal stability of polymer/clay nanocomposites at the initial stage of the degradation (before 400°C) is reduced nearly to 80°C, which can be because of the clay catalytic effects on the degradation of PP.[23,24] At temperatures higher than 400°C, PP/clay nanocomposites are more stable than pure PP which must be due to clay barrier properties domination to its catalytic effects.[24] However, due to the clay catalytic effects, at high clay loading (e.g. 10%), the onset temperature of PP/clay nanocomposite and thermal stability decreases compared with PPCNC 3.3%.

CONCLUSIONS

PPCNC were successfully prepared via *in situ* polymerization of propylene by $MgCl_2$/Clay bisupported Zeigler-Natta catalyst. Obtained results show that the polymerization temperature, H_2 concentration, and Al/Ti molar ratio have direct effects on the prepared product and polymerization yield. XRD patterns, TEM, and SEM images of prepared composites illustrate intercalation and exfoliation of the clay layers and probably good adhesion between polypropylene matrix and silicates layers. Obtained results from DSC analysis showed increase in melting and crystallization temperature, and reduction in crystalinity of prepared nanocomposites. Reduction in permeability and increase in the thermal stability of the prepared PP/clay nanocomposites also confirm the preparation of an intercalated and exfoliated structure.

References

1. Pinnavaia, T. J.; Beall, G. W. Polymer-Clay Nanocomposits; Wiley: New York, 2000; pp 97–109.
2. Hwu, J. M.; Jiang, G. J Appl Polym Sci 2005, 95, 1228.
3. Hambir, S.; Bulakh, N.; Jog, J. P. Polym Eng Sci 2002, 42, 1800.
4. Chang, J. H.; Kim, S. J.; Joo, Y. L.; Im, S. Polymer 2004, 45, 919.
5. He, A.; Wang, L.; Li, J.; Dong, J.; Han, C. C. Polymer 2006, 47, 1767.
6. Rong, J.; Li, H.; Jing, Z.; Hongm, X.; Sheng, M. J Appl Polym Sci 2001, 83, 1829.
7. Rong, J.; Sheng, M.; Li, H. Polym Compos 2002, 23, 658.
8. Utraki, L. A. Clay Containing Polymeric Nanocomposites; Rapra Technology: Crewe, UK, 2004; Vol. 2, pp 3–85.
9. Utraki, L. A. Clay Containing Polymeric Nanocomposites; Rapra Technology: Gewe, UK, 2004; Vol. 2, pp 470–505.
10. Wang, K. H.; Choi, M. H.; Koo, C. M.; Choi, Y. S.; Chung, I. J Polym 2001, 42, 9819.
11. Ramazani, S. A.; Tavakolzadeh, F.; Baniasadi, H. Polym Compos, to appear.
12. Ma, J.; Qi, Z.; Hu, Y. J Appl Polym Sci 2001, 82, 3611.
13. Gao, M.; Lio, H.; Wang, J.; Li, C.; Ma, J.; Wei, G. Polymer 2004, 45, 2175.
14. Ramos, J.; Cruz, V.; Munoz, A.; Martinez, J. Polymer 2000, 41, 6161.
15. Liu, B.; Murayama, N.; Terano, M. Ind Eng Chem Res 2005, 44, 8.
16. Zohuri, G. H.; Azimfar, F.; Jamjah, R.; Ahmadjo, S. J Appl Polym Sci 2003, 89, 1177.
17. Alexandre, M.; Dubois, P.; Sun, T.; Garces, J. M.; Jerome, R. Polymer 2002, 43, 2123.
18. Kuo, S. W.; Huang, W. J.; Huang, S. B.; Kao, H. C.; Chang, F. C. Polymer 2003, 44, 7709.
19. Garcia, M.; Van Zyl, W. E.; Ten Cate, M. G. J.; Stouwdam, J. W.; Verweij, H.; Pimplapure, M. S.; Weickert, G. Ind Eng Chem Res 2003, 42, 3750.
20. Ma, J.; Zhang, S.; Qi, Z.; Li, G.; Hu, Y. J Appl Polym Sci 2001, 83, 1978.
21. Mark, J. E. Polymer Data Hand Book; Oxford University press: New York, 1999; p 782.
22. Zhang, Y. Q.; Lee, J. H.; Rhee, J. M.; Rhee, K. Y. Compos Sci Technol 2004, 64, 1383.
23. Qin, H.; Zhang, S.; Zhao, C.; Feng, M.; Yang, M.; Shu, Z.; Yang, S. Polym Degrad Stab 2004, 85, 807.
24. Zhao, C.; Qin, H.; Gong, F.; Feng, M.; Zhang, S.; Yang, M. Polym Degrad Stab 2005, 87, 183.